*Journal of Thermal Analysis, Vol. 32 (1987) 883–891*

# THERMAL DECOMPOSITION OF AMMONIUM PERMANGANATE*

*F. M. Radwan, A. M. Abd El-Hameed, M. R. Mahmoud**** and *R. B. Fahim*****

DEPARTMENT OF CHEMISTRY, FACULTY OF SCIENCE,
SUEZ CANAL UNIVERSITY, ISMAILIA;
***DEPARTMENT OF CHEMISTRY, FACULTY OF SCIENCE, MINIA
UNIVERSITY, EL-MINIA, EGYPT

(Received June 10, 1986)

The parent material, ammonium permanganate, was carefully decomposed in air at 120°. The product, referred to as the starting material (SM), was then subjected to thermal treatment in air for 5 hr in the temperature range 150–1200°. Chemical analysis of SM indicated that the main decomposition product of $NH_4MnO_4$ was $Mn_2O_3$, together with $MnO_2$, $NH_4NO_3$, $H_2O$ and $O_2$. $Mn_3O_4$ started to form at 900°. The infrared spectra of various calcination products revealed the retention of $NH_4^+$ in the lattice structure up to 300°, and reflected the presence of excess oxygen as coordinated $O_2^-$. The TG, DTA and IRA results on SM supported the chemical analysis data. X-ray analysis was carried out for phase identification and to follow transformations and the formation of a solid solution between $MnO_2$ and $Mn_2O_3$.

In the literature, studies devoted to the thermal decomposition of ammonium permanganate are rare. Bircumshaw and Tayler [1] studied the explosion of $NH_4MnO_4$ under vacuum in the temperature range 70–111° in an inert oil. They concluded that the oil prevented contact between the individual crystals and damped self-heating effects, and that the decomposition products were $MnO_2$, $Mn_2O_3$, $NH_4NO_3$, $H_2O$, $N_2$, $O_2$, $NO_2$ and $N_2O$. Pavlyuchenko et al. [2] showed that decomposition was slow at $\leqslant 90°$, very fast at $\geqslant 96°$, and explosive at $\geqslant 100°$. They identified $MnO_2$, $MnO$, $O_2$, $H_2O$, $NO_2$, $NO$ and $NH_3$ as thermal decomposition products.

The aim of the present investigation was to characterize the calcination products of $NH_4MnO_4$ as a precursor for manganese oxide catalysts. This was performed through both chemical analysis and a number of physical tools.

* Paper presented at the World Conference on Thermal Analysis, Madeira (Portugal), 1986.

** Department of Chemistry, Faculty of Science, Assiut University Assiut, Egypt.

*John Wiley & Sons, Limited, Chichester*
*Akadémiai Kiadó, Budapest*

## Experimental

### *Materials*

Ammonium permanganate was prepared according to the method given by Bircumshaw and Tayler [1]. The long purple needle crystals of $NH_4MnO_4$ were carefully decomposed by feeding through an air condenser into a 1-litre flask placed in a drying oven at 110°. The product was further heated in situ for 2 hr at 120°, to give the starting material (SM). This was followed by the heating of SM for 5 hr in air at 150, 300, 450, 750, 900, 1000 or 1200°.

## Chemical analysis

Chemical analyses of the calcination products for $MnO_2$, $Mn_2O_3$, total manganese content and hence $Mn_3O_4$ were carried out according to standard methods [3]. Active oxygen and excess surface oxygen were determined according to the method given by Selwood [4] and by the wet hydrazine method [5], respectively.

### *Apparatus and techniques*

X-ray diffraction analysis was carried out with a Philips X-ray diffractometer (P.W. 1050/25) with Ni-filtered $CuK_\alpha$ radiation ($\lambda = 1.542$ Å). The unit cell dimension of pure cubic $\alpha$-$Mn_2O_3$ was elucidated via $a = d\sqrt{h^2+k^2+l^2}$, where $a$ is the unit cell dimension, $d$ is the interplanar diffraction line distance and ($hkl$) are the indices of the plane. The corrected unit cell dimension ($a_0$) was obtained by Cohen's least-square extrapolation method [6, 7]. Infrared measurements were carried out on a Perkin–Elmer 580 B spectrophotometer, using the KBr technique.

Thermogravimetric (TG) and differential thermal Analysis (DTA) curves were recorded automatically over a wide range of temperatures (RT–1200°), at a low rate of heating (5 deg/min) and in a dynamic atmosphere of air (20 ml/min), using small portions of the test sample (5 mg), as described earlier [8].

## Results and discussion

### *Chemical and infrared analyses*

Table 1 presents the chemical analysis data on the various calcination products of $NH_4MnO_4$ in the temperature range 120–1200°, and the corresponding significant

**Table 1** Chemical analysis data of the starting material (SM) and the various calcination products

| Sample at | $MnO_2$ % | $Mn_2O_3$ % | $Mn_3O_4$ % | Total Mn, % | | Excess surface oxygen mg/g | Active oxygen, % | | Loss on ignition % |
|---|---|---|---|---|---|---|---|---|---|
| | | | | found | calc. | | found | calc. | |
| SM | 14.58 | 73.15 | — | 60.12 | 60.33 | 21.96 | 10.07 | 9.95 | 16.72 |
| 150 °C | 32.05 | 58.15 | — | 60.87 | 61.15 | 33.80 | 11.57 | 11.64 | 12.51 |
| 300 °C | 45.11 | 47.03 | — | 61.75 | 61.88 | 46.41 | 12.68 | 12.61 | 10.42 |
| 450 °C | 61.54 | 32.83 | — | 62.38 | 62.60 | 19.61 | 14.19 | 14.03 | 7.56 |
| 600 °C | 54.60 | 40.40 | — | 62.88 | 63.40 | 18.16 | 14.01 | 13.59 | 6.84 |
| 750 °c | 38.58 | 65.63 | — | 64.42 | 64.34 | 10.65 | 12.90 | 12.45 | 6.60 |
| 900 °C | 5.60 | 66.99 | 25.39 | 67.38 | 67.83 | 6.65 | 9.74 | 9.61 | 2.73 |
| 1000 °C | — | — | 97.28 | 70.10 | 70.10 | 4.16 | 7.8 | 6.82 | — |

infrared bands are given in Table 2. The results on SM show that the main decomposition product of $NH_4MnO_4$ is $Mn_2O_3$, together with $MnO_2$, $NH_4NO_3$, $H_2O$ and $O_2$. These results are consistent with those described previously [1]. With rise of the calcination temperature in the range 120–450°, the $MnO_2$ content increases at the expense of $Mn_2O_3$, while on further heating the reverse takes place [9, 10]. The formation of $Mn_3O_4$ at $\geqslant 900°$ is in accordance with the fact that, when heated in air to about 1000°, all oxides of manganese form $Mn_3O_4$ [11].

The infrared spectra of the calcination products in the temperature range 120–300° indicate the presence of $NH_4^+$, which is probably retained in the oxide structure [12]. This is deduced from the appearance of the N—H stretching vibrations in the range 3200–3500 $cm^{-1}$ and the NH deformation at 1382 $cm^{-1}$ [13] (Table 2). These characteristic infrared bands for $NH_4^+$ are not present in the infrared spectra recorded for the calcination products obtained above 300°. This can be attributed to its dissociation to $N_2O$ and water vapour [14]. In addition, the infrared spectra of the calcination products are characterized in most cases by a well-defined band at 1200 $cm^{-1}$ (Fig. 1, Table 2). Since $O_2^-$ exhibits a characteristic band at 1097 $cm^{-1}$ [15], the band shifted to 1200 $cm^{-1}$ can be tentatively assigned to the presence of $O_2^-$ in a coordinated form. The unexpected shift to higher frequency can be attributed to the fact that the coordinated electrons of $O_2^-$ are of an antibonding character. A similar assignment for coordinated $O_2^-$ at 1140 $cm^{-1}$ has been reported by several authors [16–18]. Further evidence for the coordinated character of the $O_2^-$ was obtained from EPR measurements on the calcination product at 300° (maximum value of excess surface oxygen—Table 1), which proved to be silent.

It can be observed that the chemical analysis data on the various calcination products studied accord with those obtained from the corresponding infrared spectra. In the temperature range 120–750°, the presence of the two oxides $MnO_2$

**Table 2** Assigment of the significant bands ($cm^{-1}$) of the infrared spectra of the SM and the various calcination products

| SM | 150 °C | 300 °C | 450 °C | 600 °C | 750 °C | 900 °C | 1000 °C | 1200 °C | Assignment |
|---|---|---|---|---|---|---|---|---|---|
| 3200–3500 (sb) | 3200–3500 (sb) | 3300–3500 (sb) | — 3450 (mb) | — 3450 (mb) | — — | — | — | — | NH and O—H stretching; $\gamma$-$MnO_2$ [20] |
| 1382(s) | 1382(s) | 1382(s) | — | — | — | — | — | — | NH deformation |
| 1200(s) | 1200(s) | 1200(s) | — | — | — | 1200(m) | 1200(m) | 1200(vs) | Coordinated $O_2^-$ |
| 1030(wb) | — | — | — | — | 1030(wb) | — | — | — | $\gamma$-$MnO_2$ [19] |
| — | — | — | 680(sh) | 680(sh) | 680(sh) | — | — | — | $\gamma$-$MnO_2$ [19, 20] |
| — | — | — | — | — | — | 610(vs) | 628(vs) | 628(vs) | $Mn_3O_4$ [24, 26] |
| 570(sh) | 570(sh) | 570(sh) | 575(m) | 575(m) | 575(s) | — | — | — | $\gamma$-$MnO_2$ [21] and $\alpha$-$Mn_2O_3$ [22, 23] |
| — | — | — | — | — | — | 520(vs) | 525(vs) | 525(vs) | $Mn_3O_4$ [24, 26] |
| 525(m) | 525(m) | 520(m) | 525(m) | 520(m) | 525(m) | — | — | — | $\alpha$-$Mn_2O_3$ [22–24] and $\gamma$-$MnO_2$ [19] |
| — | — | — | — | — | — | — | 420(vs) | 420(vs) | $Mn_3O_4$ [24, 26] |
| 415(w) | 415(w) | 415(w) | 415(w) | — | — | | | | $\alpha$-$Mn_2O_3$ [23] |
| 370(w) | 370(w) | 372(w) | 370(w) | 370(w) | 370(w) | 362(m) | — | — | $\alpha$-$Mn_2O_3$ [23] |
| — | — | — | — | — | — | — | 350(s) | 352(vs) | $Mn_3O_4$ [26] |
| 348(w) | 348(w) | 348(w) | 348(w) | 348(w) | 348(w) | | | | $\alpha$-$Mn_2O_3$ [25] |
| 320(w) | 320(w) | 320(w) | 320(w) | 320(w) | 320(w) | — | — | — | $\alpha$-$Mn_2O_3$ [23] |
| 297(w) | 297(w) | 297(w) | 297(w) | 300(w) | 300(w) | 297(w) | — | — | $\alpha$-$Mn_2O_3$ [23, 25] |
| | | | | | | | | 240(m) | $Mn_3O_4$ distortion from Cubic symmetry [27, 28] |

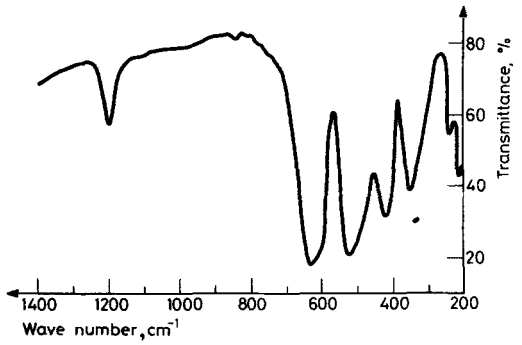


**Fig. 1** Infrared spectrum of the calcined product at 1200°

[19–21] and $Mn_2O_3$ [22–25] can be detected (cf. Table 2). On the other hand, the infrared spectrum for the decomposition product at 900° shows the characteristic bands of both $Mn_2O_3$ and $Mn_3O_4$ [24, 26–28] (cf. Table 2). At 1000° and 1200° the decomposition product appears to be pure $Mn_3O_4$ (Fig. 1).

*DTA and TG*

Figure 2 depicts the TG curve of SM, the 120° thermal decomposition product of $NH_4MnO_4$. The curve shows a smooth weight loss over the wide temperature range 105–415°, followed by a rather slow one in the temperature range 415–835°. The first overall weight loss (5.5%) can be ascribed to a weight compromise between an increase due to the transformation of $Mn_2O_3$ to $MnO_2$ (~4.1%) and a loss of surface excess oxygen (0.23%), as well as that corresponding to water removal (4.2%, calculated from the loss on ignition) and $NH_4NO_3$ elimination (5.91%, calculated by difference). The removal of water and $NH_4NO_3$ in this temperature

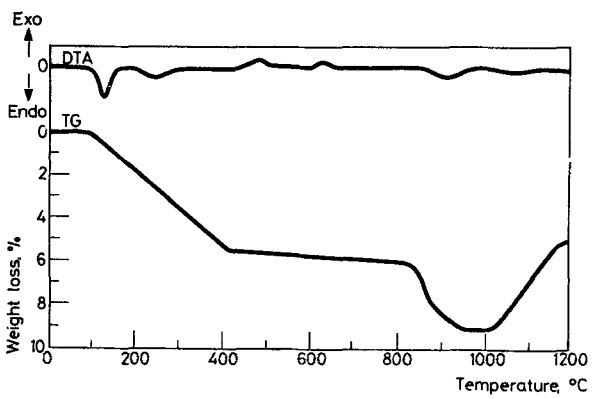


**Fig. 2** DTA and TG curves of the starting material

range is substantiated by the endothermic effect at 125° and the broad one centred at 250°, respectively, in the corresponding DTA curve given in Fig. 2. The second, slow weight loss (0.6%) can be taken to correspond to the decomposition of $MnO_2$ to $Mn_2O_3$ [9, 10], as is reflected by the chemical analysis data in Table 1. However, the disagreement between this recorded weight loss and the calculated one (2.1%), due to the transformation of ~25% of $MnO_2$ to $Mn_2O_3$, can be ascribed to the fact that $Mn_2O_3$ absorbs oxygen without change in the lattice, to form $MnO_{1.58}$ [29].

The exothermic effect at 460° in the DTA curve can be ascribed to a crystallization process, while the second, broad exothermic effect at 610° may tentatively be ascribed to some sort of phase transformation (vide infra X-ray analysis).

In the temperature range 835–1020°, the TG curve exhibits two steps of weight loss, followed by a plateau. The first step, which is a steep one, lies in the range 835–880° (2%), corresponding to the transformation of $MnO_2$ to $Mn_3O_4$ [11]. The second one, which is relatively slow (1.1%), can be related to the transformation $Mn_2O_3 \rightarrow Mn_3O_4$ [30, 31]. This behaviour is in accordance with the data listed in Table 1. The discrepancy between the calculated weight losses (5%) and the experimental ones (3.1%) for the two steps can be ascribed to the nonstoichiometry of $Mn_2O_3$, as mentioned above [29]. In this respect it is worth mentioning that $MnO_2$ cannot take up oxygen without showing the $Mn_2O_3$ lattice [29]. The formation of $Mn_3O_4$ is reflected in the DTA curve by the appearance of a broad endothermic effect at 900°.

Finally, the TG curve shows a gradual increase in weight (4.2%) from 1020° up to 1170°, nearly reaching a plateau. This is the range of temperature where $Mn_3O_4$ would take up oxygen to give a new compound of composition $Mn_3O_{4.26}$ [29].

*X-ray analysis*

Figure 3 shows the X-ray diffraction patterns of SM and the various calcination products. From a comparison with the ASTM cards, the pattern for SM reveals the existence of $\alpha$-$Mn_2O_3$. Heating at 150° indicates the same diffraction pattern, but the intensities of the diffraction lines are slightly decreased. For the sample heated at 300°, the diffractogram reveals the three strongest lines characteristic of $\gamma$-$MnO_2$. Further, the crystallinity of $\alpha$-$Mn_2O_3$ declines and the pattern indicates the appearance of a coagglomerated phase $K_{1-2}Mn_8O_{16}$ (ASTM card 20–908). The 450° sample is composed of $\alpha$-$Mn_2O_3$, $\gamma$-$MnO_2$ and the coagglomerated phase of $MnO_2$ in a higher concentration than at 300°. The pattern indicates significant crystallization of the oxides. The calcination process at 600° reflects the appearance of $\gamma$-$Mn_2O_3$, which is tetragonal. The corresponding pattern also indicates the existence of $\gamma$-$MnO_2$ and its coagglomerated phase, with no change in its

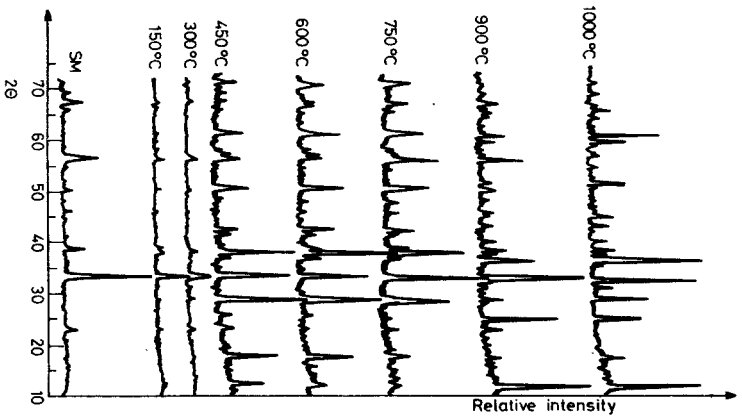


**Fig. 3** X-ray diffraction patterns of calcination products of starting material

concentration relative to that at 450°. The phase present in the 750° samples are $\alpha$-$Mn_2O_3$, $\gamma$-$Mn_2O_3$, $\gamma$-$MnO_2$ and its coagglomerated phase. The intensities of the diffraction lines characteristic of $\gamma$-$Mn_2O_3$ are lower than those at 600°. The pattern at 900° reveals the most intensive lines characteristic of $Mn_3O_4$. It also shows the presence of $\alpha$-$Mn_2O_3$ and a trace of $\gamma$-$MnO_2$. However, unidentified lines too appear, with $d$ spacings of 7.054, 3.534, 2.265 and 2.118 Å.

Finally, the X-ray diffraction pattern of the 1200° sample was identified as distorted cubic $Mn_3O_4$. This is confirmed by the appearance of an IR band for distorted cubic $Mn_3O_4$ at 240 $cm^{-1}$ in the infrared spectrum of the 1200° sample [27, 28], as shown in Fig. 2.

From the above analysis it can be concluded that SM is mainly $\alpha$-$Mn_2O_3$, which on heating gives $\gamma$-$MnO_2$, while crystallinity declines simultaneously up to 300°. Heating at 450° develops the crystallization significantly (cf. DTA curve) and the coagglomerated form of $MnO_2$. At 600° we get a significant phase transformation of the cubic $\alpha$-$Mn_2O_3$ to tetragonal $\gamma$-$Mn_2O_3$ (cf. DTA curve, Fig. 2). The corrected unit cell dimensions $a_0$ were calculated for the calcination products and were found to be:

| Sample | $\alpha$-$Mn_2O_3$ (pure) | 300° | 450° | 600° | 750° |
|---|---|---|---|---|---|
| $a_0$ Å | 9.430 | 9.418 | 9.396 | 9.430 | 9.464 |

The lower values of $a_0$ for the 300° and 450° samples as compared to that for pure $\alpha$-$Mn_2O_3$ would indicate the progress of a solid-state solution. However, the corresponding higher value for the 750° sample would also indicate solid-state solution formation through a different mechanism [32]. In this calcination product (750°), it was found that the positions of lines of $\gamma$-$MnO_2$ were shifted to lower

values of $2\theta$, i.e. their interplanar spacing values increase and the unit cell dimension increases. The $a_0$ value for the 600° sample is the same as that for pure $\alpha$-$Mn_2O_3$, suggesting the absence of a solid solution due to distortion of the cubic lattice of $\alpha$-$Mn_2O_3$, forming the tetragonal $\gamma$ phase. Solid-state formation for the 300, 450 and 750° samples was confirmed by preliminary measurements of the magnetic susceptibilities of these samples [33].

## References


1 L. L. Bricumshaw and T. M. Tayler, J. Chem. Soc., (1950) 3674.
2 M. M. Pavlyuchenko, N. G. Rafal'skii and L. A. Isybul' Ko, Geterog. Khim. Reakt., (1961) 99.
3 K. M. Pavida, S. B. Kanuogo and B. R. Sant, Electrochim. Acta, 26 (1981) 435.
4 T. E. Moore, M. Ellis and B. W. Selwood, J. Am. Chem. Soc., 72 (1950) 856.
5 M. Kobayashi, H. Matsumoto and H. Kobayashi, J. Catal., 21 (1971) 48.
6 M. U. Cohen, Rev. Sci. Instrum., 6 (1935) 68; (1936) 155.
7 J. B. Nelson and D. P. Riley, Proc. Phys. Soc. (London), 57 (1945) 160.
8 R. B. Fahim, M. I. Zaki and R. B. Gabr, Surf. Technol., 11 (1980) 215.
9 J. Ambrose, A. K. Covington and H. R. Thirsk, Trans. Faraday, Soc., 65 (1969) 1897.
10 H. Remy, Treatise on Inorganic Chemistry, Part III, Translated J. C. Anderson, ed. J. Kleinberg, 1970, p. 214.
11 J. C. Ballar, H. J. Emeleus, Sr. R. Nyholom and A. F. Trotman-Dickenson, Comprehensive Inorganic Chemistry, Part III, (1975) 1805, 798:
12 G. Butler and H. R. Thirsk, Acta Cryst., 5 (1952) 288.
13 J. B. Lambert, H. F. Shurvell, L. Verbit, R. G. Cooks and G. H. Stout, Organic Structural Analysis, Macmillan Publishing, New York, 1976, p. 235.
14 F. A. Cotton and G. Wilkinson, Advanced Inorganic Chemistry, John Wiley and Sons, New York, 1972, p. 334.
15 L. Andrews and R. Smardzewski, J. Chem. Phys., 58 (1973) 2258.
16 J. A. McGinnety, MIB, Int. Rev. Sci. Inorg. Chem., 5 (1972) 229.
17 V. J. Choy and C. H. O'Conner, Coord. Chem. Rev., 9 (1972) 45.
18 J. A. Conner and E. A. V. Ebsworth, Adv. Inorg. Radio Chem., 6 (1964) 279.
19 G. A. Kolta, F. M. A. Kerim and A. A. A. Azim, Z. Anorg. Allg. Chem., 384 (1971) 260.
20 J. B. Fernandes, B. Desai and V. N. K. Dalal, Electrochim. Acta, 28 (1983) 309.
21 F. Vranty, M. Dilling, F. Gugliotta and C. N. R. Rao, J. Sci. Ind. Res., B 20 (1961) 590.
22 G. Gattow and O. Glemser, Z. Anorg. Allg. Chem., 309 (1961) 121.
23 W. B. White and V. G. Keramidas, Spectrochim. Acta, 28A (1972) 501.
24 O. Henning and U. Strobel, Weiss Z. Hoch Arkhitekt Bauw., Weimar, 14 (1967) 645.
25 M. Parodi, Compt. Rend., 205 (1937) 906.
26 A. I. Boldyrev and A. S. Povarennykh, Zap Vses Mineral. Obshchest., 97 (1968) 3.
27 K. Siratori and Y. Aiyama, J. Phys. Soc. Japan, 20 (1965) 1962.
28 K. Siratori J. Phys. Soc. Japan, 23 (1967) 948.
29 M. LeBlanc and G. Wehner, Z. Physik. Chem., A 168 (1934) 59.
30 T. E. Moore, M. Ellis and P. W. Selwood, J. Amer. Chem. Soc., 72 (1950) 856.
31 R. Norrestam, Acta Chem. Scand., 21 (1967) 2871.
32 E. C. Kruissink, L. E. Alzamora, S. Or, E. B. M. Doesburg, L. L. Vanreijen, J. R. H. Ross and G. Van Veen; in B. Declmon, P. A. Jacobs and G. Poncelet (Eds), Preparation of Catalysts II, Elsevier, Amsterdam, 1979, p. 143.
33 J. A. Lee, C. E. Newnham, F. L. Tye and F. S. Stone, J. Chem. Soc., Farad. Trans. 1, 74 (1978) 237.

**Zusammenfassung** — Die Muttersubstanz, Ammoniumpermanganat, wurde in Luft bei 120° vorsichtig zersetzt. Das dabei erhaltene Ausgangsmaterial (SM) wurde danach in Luft 5 Stunden im Temperaturbereich von 150–1200° thermisch behandelt. Die chemische Analyse von SM ergab, daß als Hauptprodukt der Zersetzung von $NH_4MnO_4$, $Mn_2O_3$ auftritt neben $MnO_2$, $NH_4NO_3$, $H_2O$ und $O_2$. Die Bildung von $Mn_3O_4$ beginnt bei 900°. Aus Infrarotspektren verschiedener Kalzinierungsprodukte ist ersichtlich, daß in der Gitterstruktur $NH_4^+$ bis 300° zurückgehalten wird und überschüssiger Sauerstoff in Form von koordiniertem $O_2$ vorliegt. Die Ergebnisse der TG-, DTA- und IRA-Untersuchungen von SM bestätigen Daten der chemischen Analyse. Mittels Röntgenanalyse wurden die Phasen identifiziert und der Verlauf der Phasenübergänge und der Bildung einer festen Lösung zwischen $MnO_2$ und $Mn_2O_3$ verfolgt.

**Резюме** — Первоначально перманганат аммония подвергали осторожному разложению на воздухе при 120°. Получаемый при этом продукт, называемый как исходное вещество, подвергался затем в течении 5 часов термической обработке на воздухе в интервале температур 150–1200°. Химический анализ показал, что главным продуктом разложения являлась окись трехвалентного марганца, наряду с двуокисью марганца, нитратом аммония, водой и кислородом. При температуре 900° начиналось образование $Mn_3O_4$. ИК спектры различных продуктов прокаливания показали удерживание до 300° аммонний-иона в решетке и присутствие кислорода в форме $O_2^-$. Данные ТГ, ДТА и ИК спектроскопии подтвердили результаты химического анализа. Рентгеноструктурный анализ был использован для идентификации фаз, исследования превращений и образования твердого раствора между двуокисью марганца и окисью трехвалентного марганца.